A Minimal Study of the Wavelength Dependence of LWR Degradation

Albert V. Holm
Computer Sciences Corporation

ABSTRACT

The details of the wavelength dependence of the known loss of sensitivity of the Long Wavelength Redundant (LWR) camera are studied from a small subset of sensitivity monitoring observations. This analysis shows the camera has lost sensitivity at all wavelengths, but that there is a strong, broad feature centered on 2300Å where the loss is a maximum. The derived rate of change is consistent with the quick look monitoring results, but differ from laboratory-based predictions of the expected damage to the optical materials used in the spectrograph and detector. This analysis shows that the optical degradation is a strong function of both wavelength and position on the detector faceplate.

I. INTRODUCTION

When trying to compare the energy distribution of R Coronae Borealis during its recent minimum with reference spectra obtained on Christmas 1978, I concluded that some correction would have to be made for the decrease in sensitivity of the LWR during the intervening time (e.g. Sonneborn 1984). IUE's quick-look sensitivity monitoring analysis had been established to warn when sensitivity changes were becoming significant, but lacked the wavelength resolution to generate corrections to be applied to the spectra. Therefore, I undertook to determine the instrumental degradation between the two dates of interest to me while preserving the wavelength resolution present in the original spectra.

I am presenting the results here because they may be of some use outside my own research. Section II discusses the observations used and the procedure followed; Section III the results; and Section IV possible causes of the degradation.

II. DATA AND PROCEDURE

Spectra of *HD 60753, BD+28° 4211, BD+75° 325,* and *BD+33° 2642* from the IUE calibration database were used for this study. For each star only spectra having identical exposure lengths were used to minimize systematic linearity errors (eg. Oliversen 1983). Table 1 provides details of the selected observations. Nineteen large aperture point source spectra were used in this analysis. Six small aperture spectra and four trailed spectra also analyzed to check for consistency.

The detailed reduction procedure is outlined here.

1. Individual spectra were processed as follows:
   1.1. Net fluxes for the point source spectra and two of the trailed spectra were obtained from the merged spectrum file provided by IUE Spectral Image Processing System (SIPS). The IUELO procedure at the GSFC IUE Regional Data Analysis Facility (RDAF) was used for this purpose. The exceptions are the trailed spectra LWR3474 and LWR5414 which were extracted from the line-by-line file to correct for SIPS errors in the placement of the background extraction slit prior to 1980 March (Turnrose and Harvel 1982).
   1.2 Flux rates were derived using exposure durations calculated with the inclusion of quantization and camera response time effects (Schiffer 1980).
   1.3. The thermal dependence of the LWR sensitivity was removed by dividing the net flux by

$$[1.0 - 0.011 * (THDA - 12)]$$

   where the rate came from Schiffer (1982a) and the reference temperature from Bohlin and Holm (1980).

1.4. Wavelength assignments of old spectra were corrected to the mean dispersion constants (Turnrose et al 1979; Thompson et al 1980) using the technique of Schiffer (1982b). The modification in the centering of the target in the aperture described by Turnrose et al (1979) was taken into account for this correction. Because I don't know the date on which the change in centering became effective at at the VILSPA ground station, no VILSPA spectra from 1979 were used in this study.

1.5. The sampling frequency of spectra processed on the 1980 November version of IUE SIPS was artificially degraded to that of the spectra processed with the previous system by summing adjacent samples and assigning the mean wavelength to the result.

1.6. All fluxes were interpolated to a common wavelength scale by using the standard spline interpolation routine at the RDAF.

1.7. Spectral regions badly contaminated by microphonics were eliminated either by interpolation of fluxes across the affected region (for LWR16619 and LWR16589) or by deletion of the region during averaging with other spectra (for LWR16139 and LWR16587).

2. Spectra taken at nearly the same epoch were averaged. The spectra included in each average are identified in Table 2.

3. A change of sensitivity in magnitudes per year was determined from the ratios of each pair of averaged spectra identified in Table 2. In this step, the change in sensitivity was assumed to be a linear function of time. This assumption is consistent with the quick-look sensitivity monitoring analysis (Sonneborn 1984). *Hereafter the wavelength-dependent change of sensitivity in magnitudes per year will be refered to as the degradation curve.*

4. Mean degradation curves were determined separately for large aperture point source spectra, for small aperture spectra, and for trailed spectra. In this averaging, the individual degradation curves were weighted by the product of the number of spectra involved and the time interval between the reference epoch spectra and the current epoch spectra.

III. RESULTS

Figure 1 shows the individual degradation curves as determined from each of the large aperture point source ratios identified in Table 2. While the individual ratios are noisy, two common characteristics can be seen: the tendancy for degradation to be largest near the 2000Å end of the spectrum and the presence of a broad feature near 2300Å where the degradation has a maximum. These characteristics show up most clearly in the weighted mean plotted at the bottom of Figure 1. Other broad features may exist, for example, near 2840Å, but if so, they are near the noise level in these data.

Figure 2 shows the individual and mean degradation curves derived from the trailed spectra and the small aperture spectra. The 2300Å feature in the mean degradation curve derived from trailed spectra is not as deep or as narrow as in the curve from the large aperture point source. This can be seen best in Figure 3 which shows the mean curve for each of the types of spectrum. However, far fewer spectra are used in defining these curves than for the study of large aperture point source. Accordingly, it might be expected that reproducibility errors will have a larger effect in masking the systematic sensitivity changes and may be responsible for the difference in appearance. Still, all five of the individual degradation curves from point source spectra show some feature at 2300Å while none of the individual curves from trailed source spectra do. Since Oliversen (1983) finds that the reproducibility for LWR trailed spectra is a least as good as for LWR point source data, I have some concern that the difference in degradation curves is real.

In addition to the small amount of data analyzed, the small aperture degradation study has two complications. First, because of the uncertainty in the throughput of the small aperture for any observation, there can be a zero point offset in the ratio. This was corrected by normalizing the small aperture degradation curves in the 2300–3000Å bandpass to the mean curve for large aperture point source spectra. The second complication in the small aperture study is that in late 1979 the IUE project systematically began to overexpose the small-aperture sensitivity-monitoring spectra to obtain data which had better signal to noise characteristics shortward of 2600Å. This overexposure (indicated by the X's in Figure 2) eliminated any information on the sensitivity change in the 2600–2800Å bandpass. The overexposure also moved the

signal into a different region of the Intensity Transfer Function (ITF) and, therefore, allows a possibility of linearity errors (eg. Oliversen 1983). Despite these problems, the shape of the mean small aperture degradation curve shortward of 3000Å agrees well with the large aperture curve.

The validity of these results can be checked by averaging the derived degradation curves over the bandpasses used by the quick-look sensitivity monitoring program (Sonneborn 1984). The results of this check, expressed in terms of percentage sensitivity change per year, are given in Table 3. For large aperture point source spectra, there is fair agreement between the two studies, especially when allowance is made for the effects of reproducibility errors on this study which used only 19 spectra compared with the 260 spectra used by Sonneborn.

IV. DISCUSSION

The measured degradation curves do not agree with the expected wavelength dependence of the radiation-induced optical degradation of the materials in the instrument. Likely candidates for optical degradation are magnesium fluoride, which forms the entrance window of the ultraviolet-to-visible image converter (UVC), and silicon dioxide, which coats the 45° and collimator mirrors to suppress the second-order spectrum (Boggess et al. 1978). Laboratory and Orbiting Astronomical Observatory studies show that these materials develop absorption bands after irradiation by significant amounts of particle radiation. Magnesium fluoride develops a strong band centered at 2500Å (Heath and Sacher 1966) and silicon dioxide develops one centered at 2200Å (Navach and Meade 1976). Figure 4 shows how the LWR degradation differs from the the optical degradation curves for both these materials. As a confirmation of this difference an analytical Gaussian function was fitted empirically to the observed degradation curve. That function, which has the form

$$-0.023e^{-(((\lambda - 2304)/58.9)^2/2)} + 1.07x10^{-11}\lambda^2 + 1.11x10^{-5}\lambda - 0.043,$$

is illustrated in Figure 5. This function shows quantitatively that the 2300Å feature really occurs at that wavelength and that the sensitivity is decreasing toward shorter wavelengths.

A third conceivable source of the degradation is irradiation-induced changes to the quantum efficiency of the cesium tellurium photocathode, but Heath and McElaney (1968) have shown the effects of irradiation on cesium tellurium are much smaller than on magnesium flouride. Thus, the IUE measurements are not explained by laboratory studies of radiation damage in materials.

A potential solution to the difference between the observed and expected wavelength dependence of the optical degradation can be found in the report by Ake (1982) on the sensitivity change for high dispersion spectra. Figure 3 of Ake's report which shows that the contours of equal change are not parallel to the echelle orders. This demonstrates that the degradation is not solely a function of wavelength but is highly dependent on location in the LWR image. In particular, the loss of sensitivity is greatest on the left edge of the image from which an arm of low sensitivity extends diagonally toward the upper right. Furthermore, that low sensitivity arm crosses the location of the low dispersion spectrum at about 2300Å. Thus it seems likely that the 2300Å feature in the low dispersion spectrum is an artifact of the dependence of the degradation on location. Quantitatively there is reasonable agreement. My analysis gives the rate of loss of sensitivity at the 2300Å as -3.7 percent/year while Ake's high dispersion analysis gives -3.2 ± 0.7 percent/year for the corresponding location.

More information on the nature of the loss of sensitivity can be obtained from flat field images, where a Hg lamp has been used to flood the camera's faceplate with light predominantly at 2537Å. The absolute levels of these flat field images cannot be used to study camera sensitivity because the calibration lamps show time-dependent output level changes. But it is possible to compare how the the relative response of the camera in different locations varies with time. The images used for this analysis were taken from sequence of images obtained in March 1978 for construction of the LWR ITF and from the sequence obtained in November 1983 for construction of an improved ITF. Two flood images and a null image were selected from each epoch. One set of flood images (LWR1202 and LWR17034) were low level exposures

using a 37 second integration. The second set were high level exposures using a 112 second (LWR1212) or a 131 second (LWR17034) integration. The difference in integration between LWR1212 and LWR17034 was chosen deliberately to have approximately the same DN level on both images. The null images were LWR1213 and LWR17022. The first step in this analysis was to determine the mean intensity level in an area of 36x36 pixels centered on three locations on each image. These locations lie near the low dispersion spectrum at 2700Å and at 2300Å and near the left edge of the image where the analysis of high dispersion spectra showed a region of maximum degradation. Their image line and sample coordinates were (360,504), (276,360), and (432,168) respectively. Next the mean intensity from the appropriate location of the null image was subtracted from the flat field means to give a net intensity. For each image the relative sensitivity at the 2300Å and the left edge locations relative to the 2700Å location was found by dividing the net intensity at each location by the net intensity at the 2700Å location. Finally the percentage change per year was found by comparing these relative sensitivities for the two epochs and dividing by the 5.68 year time interal. *The results, summarized in Table 4, are that the flat field does not show the location dependence of degradation at the 5 to 10 σ level!* That the location dependence of degradation of the response of the camera to spectra is much greater than to 2537Å light is confirmed by an independent study by Imhoff and Heckathorn (1984).

The absence of the location dependence effect from the 2537Å images and its presence in the spectral images implies that there is a strong wavelength dependence to the loss of sensitivity or that the degradation occurs in a component which is not illuminated by the flood lamps. This in turn implies that the source of the degradation is in the optical path or in the UVC section of the camera rather than in the secondary electron conduction (SEC) vidicon section of the camera which sees only the blue light from the UVC phosphor. Therefore, the prognosis for the derivation of a suitable correction algorithm is much more favorable than if the changes had occurred in the SEC section where exposure level effects might be important.

Sonneborn's (1984) quick-look sensitivity monitoring of the Long Wavelength Prime (LWP) camera shows that the response of the LWP to spectra does not seem to be changing as rapidly as the response of the LWR. This observation further isolates the location of the optical degradation to the UVC section or to the reflectance of the camera select mirror. However, this conclusion should be regarded as tentative until the LWP degradation is analyzed both in high dispersion and in low dispersion with the technique used here.

V. CONCLUSIONS

Analysis of stellar spectra and of flat fields illuminated by the Hg flood lamps has shown that there is a loss of sensitivity which shows both wavelength and locational dependence. These characteristics indicate that optical degradation is occurring in the optical elements of the spectrograph or at the UVC section of the camera. However, because of the positional dependence of the degradation, the observed wavelength dependence does not match that of radiation damage to any of the expected optical materials.

I recommend that further analysis of the degradation using high dispersion spectra and trailed spectra be given high priority. I also recommend that the techniques described here be applied to the complete database of low dispersion sensitivity monitoring spectra for all three operational cameras.

I would like to express my appreciation of the IUE science operations staffs at Goddard and at VILSPA for their efforts in obtaining the spectra which were used in this analysis. I also want to thank Rick Wasatonic for computational assistance. This work was supported in part by NASA grant NAS 5-25774.

REFERENCES

Ake, T.B. 1982, NASA IUE Newsletter **19**, p. 37.

Boggess, A., et al. 1978, Nature **275**, 372.

Bohlin, R., and Holm, A. 1980, NASA IUE Newsletter **10**, 37.

Heath, D.F., and Sacher, P.A. 1966, Appl. Opt. **5**, 937.

Heath, D.F., and McElaney, J.H. 1968, Appl. Opt. **7**, 2049.

Imhoff, C.L., and Heckathorn, J.N. 1984, private communication.

Navach, C., and Meade, M.R. 1976, Wisconsin Astrophysics No. 28.

Oliversen, N.A. 1983, NASA IUE Newsletter **23**, p. 31.

Schiffer, F.H., III, 1980, NASA IUE Newsletter **11**, p. 33.

Schiffer, F.H., III, 1982a, NASA IUE Newsletter **19**, p. 33.

Schiffer, F.H., III, 1982b, *"Data Analysis Procedures for the International Ultraviolet Explorer Regional Data Analysis Facility. Part 1. Guidelines for Determining Wavelengths and Fluxes from Extracted Spectra"*, CSC/TM-82-6207.

Sonneborn, G. 1984, NASA IUE Newsletter **24**, p. 67.

Thompson, R., Bohlin, R., Turnrose, and Harvel, C. 1980, NASA IUE Newsletter **11**, p. 10.

Turnrose, B., Bohlin, R., Holm, A., and Harvel, C. 1979, NASA IUE Newsletter **6**, p. 180.

Turnrose, B.E., and Harvel, C.A. 1982, NASA IUE Newsletter **17**.

TABLE 1
SPECTRA USED TO STUDY LWR DEGRADATION

TARGET	IMAGE	TYPE	EXPOSURE (sec)	THDA (degrees)	DATE	COMMENT
HD 60753	LWR 2941	lg	6.84	11.8	1978/343	
	LWR 3269	"	"	12.8	1978/359	
	LWR16589	"	"	14.5	1983/226	Microphonics near 2840A
	LWR16907	"	"	15.9	1983/274	
	LWR 2941	sm	11.76	11.8	1978/343	
	LWR 3269	"	"	12.8	1978/359	
	LWR16589	"	20.77	14.5	1983/226	Overexposed; ping
	LWR 3474	tr	31.25	11.8	1979/013	4 passes
	LWR17250	"	31.25	15.4	1984/044	
+28 4211	LWR 3128	lg	59.68	13.9	1978/343	
	LWR 3286	"	"	13.2	1978/360	
	LWR 5225	"	"	12.5	1979/213	
	LWR 5337	"	"	12.8	1979/225	
	LWR15071	"	"	16.2	1983/019	Microphonics near 2880A
	LWR15077	"	"	14.5	1983/019	
	LWR16139	"	"	12.5	1983/163	Microphonics near 3060A
	LWR16587	"	"	14.2	1983/226	Microphonics near 2710A
+33 2642	LWR 3171	lg	189.52	12.5	1978/349	
	LWR16619	"	"	15.2	1983/230	Microphonics near 2940A
+75 325	LWR 5338	lg	23.64	12.5	1979/225	
	LWR 5727	"	"	12.5	1979/274	
	LWR14973	"	"	16.5	1983/001	
	LWR15362	"	"	14.5	1983/054	Microphonics near 3350A
	LWR 5338	sm	39.61	12.5	1979/225	
	LWR 5727	"	54.77	12.5	1979/274	
	LWR14973	"	71.56	16.5	1983/001	Overexposed
	LWR 5414	tr	74.10	12.2	1979/233	
	LWR14760	"	74.30	14.2	1982/335	

TABLE 2
RATIOED SPECTRA

LABEL	TARGET	TYPE	IMAGES RATIOED	TIME INTERVAL (years)	WEIGHT
A	HD 60753	lg	(LWR16589+16947)/(LWR2941+3269)	4.73	18.92
B	+28 4211	"	(LWR16139+16587)/(LWR3128+3286)	4.57	18.28
C	"	"	(LWR15071+15077)/(LWR5225+5337)	3.45	13.80
D	+33 2642	"	LWR16619/LWR3171	4.67	9.34
E	+75 325	"	(LWR14973+15362)/(LWR5338+5727)	3.39	13.56
F	"	tr	LWR14760/LWR5414	3.28	6.56
G	HD 60753	"	LWR17250/LWR3474	5.08	10.16
H	"	sm	LWR16589/(LWR2941+3269)	4.66	13.98
I	+75 325	"	LWR14973/(LWR5338+5727)	3.32	9.96

TABLE 3
AVERAGE SENSITIVITY LOSS RATES

CENTRAL WAVELENGTH	BAND WIDTH	SENSITIVITY LOSS RATE (PERCENT/YEAR) THIS REPORT	SONNEBORN 1978–1984.3	SONNEBORN 1978–1983.6
2400 A	300 A	−2.4	−2.4	−2.3
2600 A	100 A	−0.8	−1.4	−1.2
2900 A	300 A	−1.2	−1.4	−1.1

TABLE 4
COMPARISON BETWEEN LOW DISPERSION, HIGH DISPERSION, AND FLAT FIELD DATA

LOCATION	RATE OF LOSS OF SENSITIVITY RELATIVE TO 2700A LOCATION LOW DISP	HIGH DISP	Hg LAMP LOW LEVEL	Hg LAMP HIGH LEVEL
2300A	2.4	1.4 +0.7	0.0 +0.8	−0.5 +0.4
left edge	...	4.2 +0.7	0.8 +0.8	−0.2 +0.4

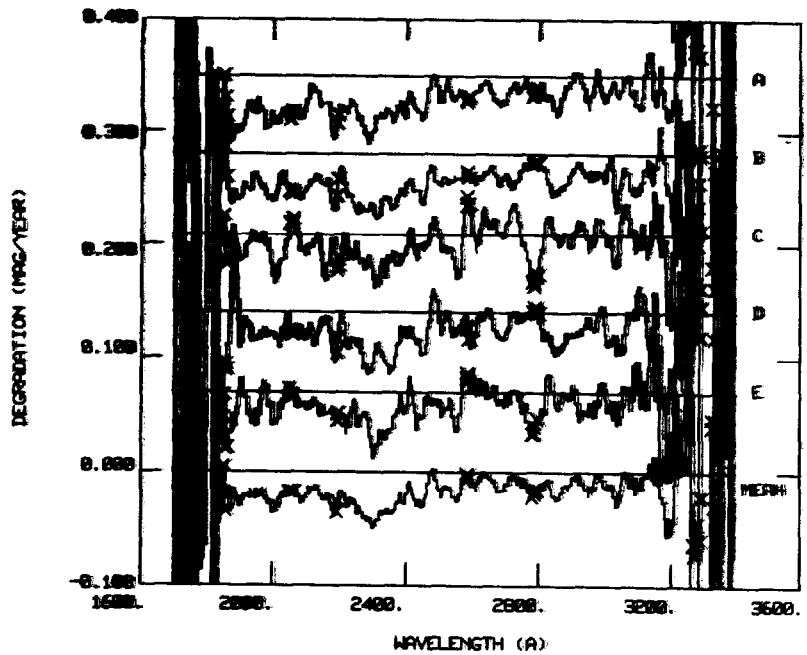

Figure 1- Individual and mean degradation curves derived from ratios of large aperture point source spectra. The letters label the individual ratios according to the identifications given in Table 2. Two tendancies to note are the maximum in the degradation near 2300Å and the general increase of degradation toward shorter wavelengths.

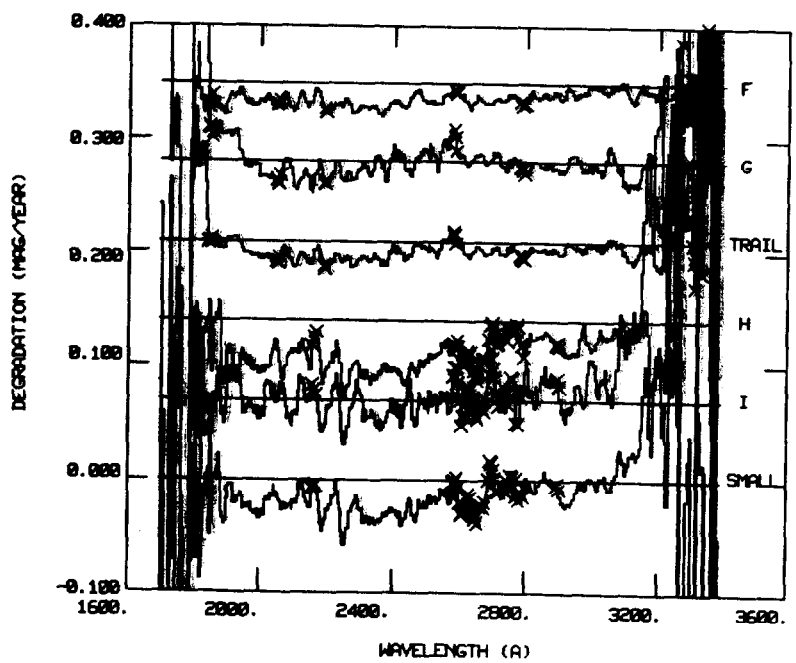

Figure 2- Individual and mean degradation curves derived from ratios of trailed spectra and from small aperture spectra. The letter labels on the individual ratios refer to the identifications given in Table 2. The mean small aperture ratio is normalized to match the mean large aperture point source ratio in the 2300–3000Å bandpass.

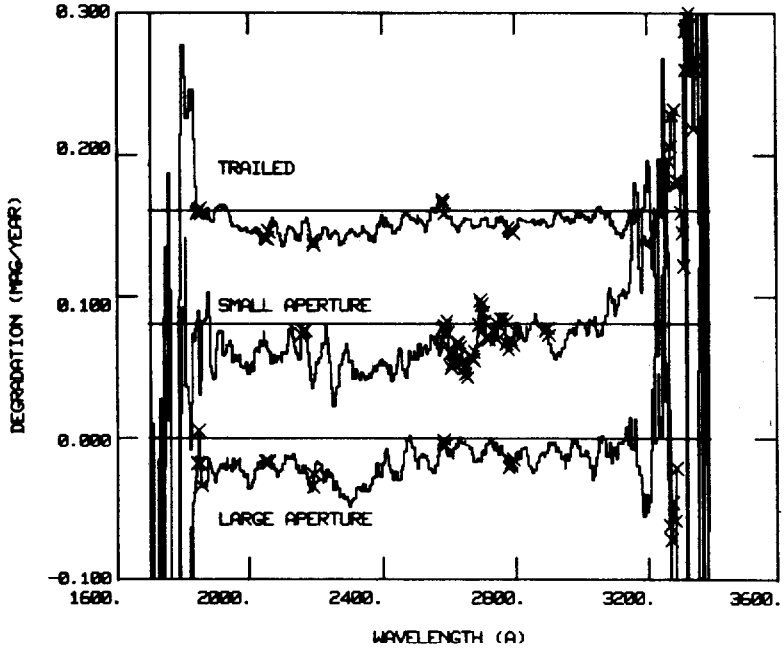

Figure 3- A comparison of the mean degradation curves for the three different classes of spectra studied in this work.

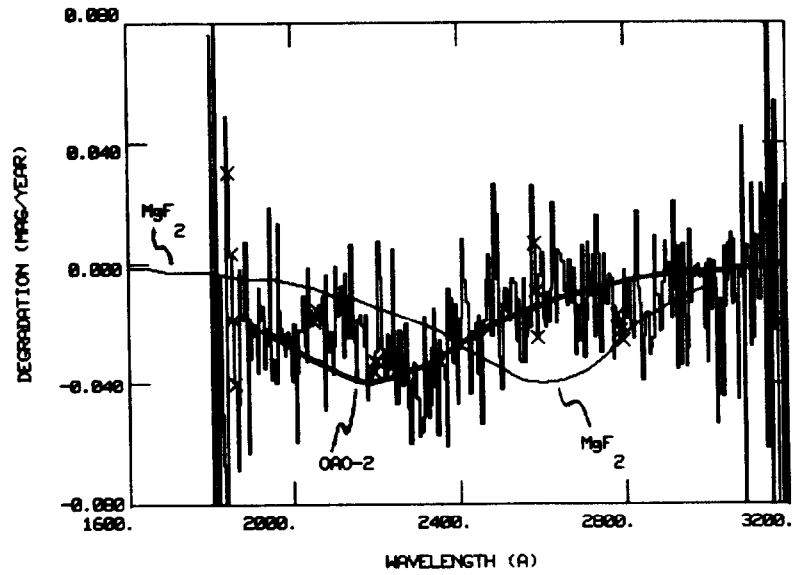

Figure 4- A comparison of the observed IUE degradation from large aperture point source spectra with the expected radiation-induced optical degradation of SiO_2 (labelled OAO-2) and MgF_2.

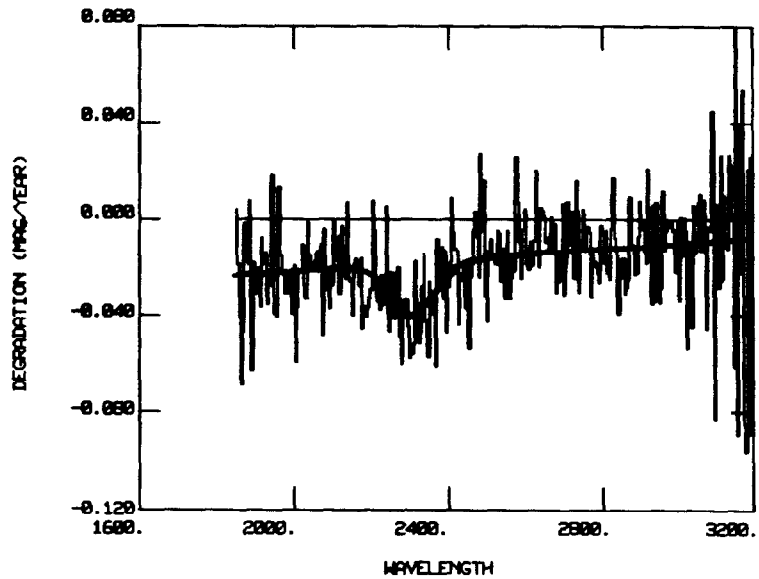

Figure 5- A comparison between the empirical analytical fit (*thick line*) to the large aperture point source degradation and the observed degradation.